Ionization time drifts for atomic $p_\pm$ orbitals in strong elliptically polarized laser fields
SUPPLEMENTARY INFORMATION

Kunlong Liu,[1] Hongcheng Ni,[2] Klaus Renziehausen,[1] Jan-Michael Rost,[2] and Ingo Barth[1]

[1] *Max-Planck-Institut für Mikrostrukturphysik, Weinberg 2, 06120 Halle (Saale), Germany*

[2] *Max-Planck-Institut für Physik komplexer Systeme, Nöthnitzer Strasse 38, 01187 Dresden, Germany*

I. THEORETICAL DERIVATIONS

In this section, we derive Eq. (4) in the paper for $G_\pm(\varphi, t)$, as well as the angle $\varphi = \varphi^\pm_{\max}$ for its local maxima, at the given time t.

A. Angular distribution of electron density

The wave functions for the initial $p_\pm$ orbitals are given by $\Psi^0_\pm(\mathbf{r}) = [\Psi_x(\mathbf{r}) \pm i\Psi_y(\mathbf{r})]/\sqrt{2}$, where the wave functions $\Psi_x(\mathbf{r}) = F(r,\theta)\cos\varphi$ and $\Psi_y(\mathbf{r}) = F(r,\theta)\sin\varphi$ are real-valued. The normalizations of $\Psi_x(\mathbf{r})$ and $\Psi_y(\mathbf{r})$ have the direct consequence for the normalization of the real-valued function $F(r,\theta)$:

$$\begin{aligned} 1 &= \int dV\ \Psi_x(\mathbf{r})^2 = \int dV\ \Psi_y(\mathbf{r})^2 \\ &= \int_0^\infty dr\ r^2 \int_0^\pi d\theta\ \sin\theta\ F(r,\theta)^2 \underbrace{\int_0^{2\pi} d\varphi\ \cos^2\varphi}_{=\pi} = \int_0^\infty dr\ r^2 \int_0^\pi d\theta\ \sin\theta\ F(r,\theta)^2 \underbrace{\int_0^{2\pi} d\varphi\ \sin^2\varphi}_{=\pi} \\ \Longrightarrow \frac{1}{\pi} &= \int_0^\infty dr\ r^2 \int_0^\pi d\theta\ \sin\theta\ F(r,\theta)^2. \end{aligned} \tag{S1}$$

Then, we can calculate the function $G^0_\pm(\varphi, t)$ via

$$G^0_\pm(\varphi, t) = \int_0^\infty dr\ r^2 \int_0^\pi d\theta\ \sin\theta\ \left|\Psi^0_\pm(\mathbf{r}, t)\right|^2, \tag{S2}$$

where the complex-valued time-dependent wave function $\Psi^0_\pm(\mathbf{r}, t)$ is given by

$$\Psi^0_\pm(\mathbf{r}, t) = \frac{1}{\sqrt{2}} e^{\Gamma^\pm_x(t)} \Psi_x(\mathbf{r}) e^{-i[E_0 t + \Phi^\pm_x(t)]} + \frac{1}{\sqrt{2}} e^{\Gamma^\pm_y(t)} \Psi_y(\mathbf{r}) e^{-i[E_0 t + \Phi^\pm_y(t)]} e^{\pm i\pi/2}. \tag{S3}$$

By defining the population $P^\pm_j(t)$, $j \in \{x, y\}$, as

$$P^\pm_j(t) = \frac{e^{2\Gamma^\pm_j(t)}}{2}, \tag{S4}$$

the phase offset $\Delta\Phi_\pm(t)$ as

$$\Delta\Phi_\pm(t) = \Phi^\pm_y(t) - \Phi^\pm_x(t), \tag{S5}$$

the population ratio $\mathcal{R}_\pm(t)$ as

$$\mathcal{R}_\pm(t) = \frac{P^\pm_y(t)}{P^\pm_x(t)}, \tag{S6}$$

and the coefficient $C_\pm(t)$ as

$$C_\pm(t) = \frac{\sqrt{P^\pm_x(t) P^\pm_y(t)}}{\pi}, \tag{S7}$$

and using Eq. (S1), we find the angular distribution of the electron density at the time t:

$$G^0_\pm(\varphi, t) = C_\pm(t) \left[\mathcal{R}^{-1/2}_\pm(t)\cos^2\varphi + \mathcal{R}^{1/2}_\pm(t)\sin^2\varphi \pm \sin\Delta\Phi_\pm(t)\sin 2\varphi\right]. \tag{S8}$$

For convenience, we omit to indicate the time t for all time-dependent quantities in the following derivation. In addition, we restrict the phase offset $\Delta\Phi_\pm$ to the interval $(-\pi, \pi]$.

B. Orbital deformation

Having derived Eq. (4) for the angular distribution $G^0_\pm(\varphi)$, we will focus on discussing where the local maxima and the minima of $G^0_\pm(\varphi)$ are located. We introduce the angle $\varphi^\pm_{\max}$, where a particular maximum of $G^0_\pm(\varphi)$ is located, and we will derive the equation for this angle, which depends on the population ratio $\mathcal{R}_\pm$ and the phase offset $\Delta\Phi_\pm$.

First, we introduce the modified phases $\tilde{\Phi}^\pm_j$, $j \in \{x, y\}$, and the modified phase offset $\Delta\tilde{\Phi}_\pm$:

$$\tilde{\Phi}^\pm_j = \pm\Phi^\pm_j, \tag{S9}$$

$$\Delta\tilde{\Phi}_\pm = \tilde{\Phi}^\pm_y - \tilde{\Phi}^\pm_x \;=\; \pm\Delta\Phi_\pm. \tag{S10}$$

Then, we rewrite Eq. (S8) for $G^0_\pm(\varphi)$ using $\sin^2\varphi = (1-\cos 2\varphi)/2$, $\cos^2\varphi = (1+\cos 2\varphi)/2$, and the definition of $\Delta\tilde{\Phi}_\pm$ as

$$G^0_\pm(\varphi) = G_\pm + \tilde{G}_\pm(\varphi), \tag{S11}$$

where the quantities $G_\pm$ and $\tilde{G}_\pm(\varphi)$ are given by

$$G_\pm = C_\pm \frac{\mathcal{R}_\pm^{-1/2} + \mathcal{R}_\pm^{1/2}}{2}, \tag{S12}$$

$$\tilde{G}_\pm(\varphi) = C_\pm \left[\frac{\mathcal{R}_\pm^{-1/2} - \mathcal{R}_\pm^{1/2}}{2}\cos 2\varphi + \sin\Delta\tilde{\Phi}_\pm \sin 2\varphi\right]. \tag{S13}$$

$G_\pm$ is independent of the angle φ but the function $\tilde{G}_\pm(\varphi)$ gives a φ-dependent contribution to the angular distribution $G^0_\pm(\varphi)$. Therefore, for the calculation of the angle $\varphi^\pm_m$, it is equivalent to analyze where the function $\tilde{G}_\pm(\varphi)$ has its local maxima instead of doing this analysis for the function $G^0_\pm(\varphi)$. In particular, the function $\tilde{G}_\pm(\varphi)$ has the property

$$\tilde{G}_\pm(\varphi) = (-1)^N \tilde{G}_\pm(\varphi + N\pi/2), \tag{S14}$$

where N indicates an integer number. Thus, due to Eq. (S14), the function $\tilde{G}_\pm(\varphi)$ is π periodic. Moreover, if there is a local extremum of $\tilde{G}_\pm(\varphi)$ for a certain angle $\varphi^\pm_e$, then we will find at all angles given by $\varphi = \varphi^\pm_e + N\pi/2$ extrema of $\tilde{G}_\pm(\varphi)$. If the extremum at the angle $\varphi^\pm_e$ is a maximum then the extrema at $\varphi = \varphi^\pm_e + N\pi/2$ will be minima for odd values of N and maxima for even values of N. It works vice versa.

Now, we make a case-by-case analysis:

(i) For the special case $\mathcal{R}_\pm = 1$ *and* $\Delta\Phi_\pm \in \{0, \pi\}$, we find just that $\tilde{G}_\pm(\varphi) = 0$. It has the consequence $G^0_\pm(\varphi) = G_\pm$, which can be interpreted as that the orbital is distributed equally for φ. Due to this reason, for this special case no local maximum $\varphi^\pm_{\max}$ of the function $\tilde{G}_\pm(\varphi)$ exists, i.e., the orbital is not polarized. This could be the case when the external field is too weak to significantly modify the population ratio or induce the Stark-shift difference between $|\Psi_{p_x}\rangle$ and $|\Psi_{p_y}\rangle$ states.

(ii) For the case $\mathcal{R}_\pm = 1$ *and* $\Delta\Phi_\pm \notin \{0, \pi\}$, we get the result $\tilde{G}_\pm(\varphi) = C_\pm \sin\Delta\tilde{\Phi}_\pm \sin 2\varphi$ with $\sin\Delta\tilde{\Phi}_\pm \neq 0$. Thus, we find in a trivial analysis that all local maxima are located at $\mathrm{sgn}(\Delta\tilde{\Phi}_\pm)\pi/4 + N\pi$ and all local minima are located at angles $-\mathrm{sgn}(\Delta\tilde{\Phi}_\pm)\pi/4 + N\pi$. We call the maximum for $N = 0$ as $\varphi^\pm_{\max}$, so this maximum is located at

$$\varphi^\pm_{\max} \;=\; \mathrm{sgn}(\Delta\tilde{\Phi}_\pm)\frac{\pi}{4}. \tag{S15}$$

(iii) In the more general case $\mathcal{R}_\pm \neq 1$, we find $\varphi^\pm_{\max}$ by analyzing the first derivative and the second derivative of $\tilde{G}_\pm(\varphi)$

$$\frac{d\tilde{G}_\pm(\varphi)}{d\varphi} = 2C_\pm \left[-\frac{\mathcal{R}_\pm^{-1/2} - \mathcal{R}_\pm^{1/2}}{2}\sin 2\varphi + \sin\Delta\tilde{\Phi}_\pm \cos 2\varphi\right], \tag{S16}$$

$$\frac{d^2\tilde{G}_\pm(\varphi)}{d\varphi^2} = 4C_\pm \left[-\frac{\mathcal{R}_\pm^{-1/2} - \mathcal{R}_\pm^{1/2}}{2}\cos 2\varphi - \sin\Delta\tilde{\Phi}_\pm \sin 2\varphi\right]. \tag{S17}$$

We obtain the polar angle $\varphi_0^\pm$ by solving $d\tilde{G}_\pm(\varphi)/d\varphi = 0$. We find:

$$-\frac{\mathcal{R}_\pm^{-1/2} - \mathcal{R}_\pm^{1/2}}{2}\sin 2\varphi_0^\pm + \sin\Delta\tilde{\Phi}_\pm \cos 2\varphi_0^\pm = 0, \tag{S18}$$

$$\Longrightarrow \tan 2\varphi_0^\pm = \frac{2\sin\Delta\tilde{\Phi}_\pm}{\mathcal{R}_\pm^{-1/2} - \mathcal{R}_\pm^{1/2}}, \tag{S19}$$

$$\Longrightarrow \varphi_0^\pm = \frac{1}{2}\arctan\frac{2\sin\Delta\tilde{\Phi}_\pm}{\mathcal{R}_\pm^{-1/2} - \mathcal{R}_\pm^{1/2}}. \tag{S20}$$

Here, the codomain of the arctan function is restricted to values $(-\pi/2, \pi/2)$. Therefore, the result given in Eq. (S20) for $\varphi_0^\pm$ is in the range of $(-\pi/4, \pi/4)$. By further analyzing the second derivative $d^2\tilde{G}_\pm(\varphi)/d\varphi^2$ at $\varphi = \varphi_0^\pm$, we have

$$\varphi_{\max}^\pm = \begin{cases} \varphi_0^\pm & \text{for } \mathcal{R}_\pm < 1, \\ \varphi_0^\pm + \dfrac{\pi}{2} & \text{for } \mathcal{R}_\pm > 1. \end{cases} \tag{S21}$$

To sum up cases (ii) and (iii), the local maximum for the angular distribution of the electron density at $\varphi_{\max}^\pm$ reads [using Eqs. (S9) and (S10)]:

$$\varphi_{\max}^\pm = \begin{cases} \pm\dfrac{1}{2}\arctan\left(\dfrac{2\sin\Delta\Phi_\pm}{\mathcal{R}_\pm^{-1/2} - \mathcal{R}_\pm^{1/2}}\right) & \text{for } \mathcal{R}_\pm < 1, \\ \pm\text{sgn}(\Delta\Phi_\pm)\dfrac{\pi}{4} & \text{for } \mathcal{R}_\pm = 1, \\ \pm\dfrac{1}{2}\arctan\left(\dfrac{2\sin\Delta\Phi_\pm}{\mathcal{R}_\pm^{-1/2} - \mathcal{R}_\pm^{1/2}}\right) + \dfrac{\pi}{2} & \text{for } \mathcal{R}_\pm > 1. \end{cases} \tag{S22}$$

The above cases (i)–(iii) tell us that if $\Delta\Phi_\pm = N\pi$, there is no maximum of the orbital (when $\mathcal{R}_\pm = 1$) or the maximum is located on either the x or y axis (when $\mathcal{R}_\pm \neq 1$); otherwise, the maximum is always located beyond the axes. During the interaction with the elliptically polarized laser field, $\Delta\Phi_\pm$ keeps being accumulated instead of being constant, so, in general, the orbitals initially carrying angular momenta would be polarized along tilted angles with respect to the ellipse of the elliptically polarized laser field.

II. NUMERICAL METHOD

A. Time-dependent Schrödinger equation

We solve numerically the three-dimensional (3D) time-dependent Schrödinger equation (TDSE) in Cartesian coordinate system for the interactions of atoms with elliptically polarized (EP) laser fields. Single-active-electron (SAE) approximation is applied. Within the dipole approximation, the length-gauge TDSE is given by (in atomic units)

$$i\frac{\partial}{\partial t}\Psi(\mathbf{r}, t) = \left[-\frac{\nabla^2}{2} + V(\mathbf{r}) + \mathbf{r}\cdot\mathbf{E}(t)\right]\Psi(\mathbf{r}, t), \tag{S23}$$

where $V(\mathbf{r})$ is effective the Coulomb potential. In particular, the potential is given by

$$V(\mathbf{r}) = -\frac{1 + 9e^{-0.85|\mathbf{r}|^{1.6}}}{\sqrt{|\mathbf{r}|^2 + 1.425}} \tag{S24}$$

for the $2p$ orbital of Ne, yielding the energy of -0.7935 a.u., and

$$V(\mathbf{r}) = -\frac{2 + 4e^{-|\mathbf{r}|} + 12e^{-0.673|\mathbf{r}|^2}}{\sqrt{|\mathbf{r}|^2 + 2e^{-1.8|\mathbf{r}|^2}}} \tag{S25}$$

for the $3p$ orbital of Ar^+, yielding the energy of -1.012 a.u. Soften-core parameters are adopted to avoid the numerical error caused by the screaming potential approaching to the origin. Note that the soften-core potential is capable of reproducing the photoelectron electron distribution measured in experiments [2]. The effective Coulomb potential for nitric oxide (NO) prealigned along the z axis can be found in Ref. [3].

The counterclockwise EP electric field is defined as

$$\mathbf{E}(t) = \mathcal{E} f(t) \left[\cos(\omega t + \phi)\mathbf{e}_x + \epsilon \sin(\omega t + \phi)\mathbf{e}_y\right], \tag{S26}$$

with the envelope function $f(t)$, given by

$$f(t) = \begin{cases} \sin^2\left(\dfrac{\pi t}{nT}\right) & \text{for } 0 \le t \le nT, \\ 0 & \text{otherwise.} \end{cases} \tag{S27}$$

In addition, $\mathcal{E}$, ϵ, ω, ϕ, n, and $T = 2\pi/\omega$ are the electric field amplitude, the ellipticity, the angular frequency, the carrier-envelope phase, the number of laser cycles, and the period of one laser cycle, respectively.

The TDSE is numerically solved using the split-operator spectral method [4]. The 3D grid ranges both for x and y from -115.2 to 115.2 a.u. and for z from -42.24 to 42.24 a.u. The grid contains $1440 \times 1440 \times 384$ grid points with the spacing steps of $dx = dy = 0.16$ a.u. and $dz = 0.22$ a.u. The time step for the evolution of the wave function is $\Delta t = 0.01$ a.u. We have tested that our simulation results are preserved for smaller time steps and larger grid ranges. For the results averaged over CEP, ϕ ranges from 0 to 2π with the step of $\pi/12$.

The initial stationary wave functions of the current-carrying orbitals are obtained by imaginary-time propagation and orthogonalization under symmetry conditions with respect to the azimuthal quantum number $m = \pm 1$. During the time evolution of the wave function, the unphysical reflections at boundaries of the calculation box are avoided by using the split function that separates smoothly the outgoing wave packet, which is then propagated analytically by using the Volkov-Hamiltonian and then contributes coherently to the final wave function $\Psi_c(\mathbf{k}, t_{\text{end}})$ in the momentum space [5]. After the pulse is off, the propagation of the wave function continues for additional five femtoseconds so that the ionized wave packet is well separated from the bound wave packet. At the end of the propagation ($t = t_{\text{end}}$), the wave packet in the area $|\mathbf{r}| < 60$ a.u. is eliminated with a smooth absorber. The remaining part of the wave function is then transferred from the position space to the momentum space. Finally, the transformed wave function is coherently added to $\Psi_c(\mathbf{k}, t_{\text{end}})$. The final 3D PMD is calculated as $Y(\mathbf{k}) = |\Psi_c(\mathbf{k}, t_{\text{end}})|^2$. The 2D PMD in the x-y plane is given by $Y^{x,y}(k_x, k_y) = \int_{-\infty}^{\infty} Y(\mathbf{k}) dk_z$. The photoelectron angular distributions (PADs) are given by $Y^{r,\varphi}(k_r(E_{\text{kin}}), \varphi) = \int_0^{\pi} Y(\mathbf{k}) k_r^2 \sin\theta d\theta$, with $k_r(E_{\text{kin}}) = \sqrt{2E_{\text{kin}}}$, and by $Y^{\varphi}(\varphi) = \int_0^{\infty} Y^{r,\varphi}(k_r, \varphi) dk_r$ after integration over the kinetic energy.

B. Three-level model

We also use three-level model to solve the TDSE

$$i\frac{\partial}{\partial t}|\Psi(\mathbf{r}, t)\rangle = \hat{H}(t)|\Psi(\mathbf{r}, t)\rangle, \tag{S28}$$

i.e. with the ansatz

$$|\Psi(t)\rangle = a(t)|\Psi_s\rangle e^{-iE_s t} + b_1(t)|\Psi_x\rangle e^{-iE_0 t} + b_2(t)|\Psi_y\rangle e^{-iE_0 t}. \tag{S29}$$

The $|\Psi_{p_x}\rangle$ and $|\Psi_{p_y}\rangle$ states and the first excited $|\Psi_s\rangle$ state above them of the selected model are considered. The time-dependent Hamiltonian is given by

$$\hat{H}(t) = \hat{H}_0 + \mathbf{r} \cdot \mathbf{E}(t), \tag{S30}$$

where $\mathbf{E}(t) = \mathcal{E}_x(t)\mathbf{e}_x + \mathcal{E}_y(t)\mathbf{e}_y$, $\hat{H}_0|\Psi_s\rangle = E_s|\Psi_s\rangle$, $\hat{H}_0|\Psi_x\rangle = E_0|\Psi_x\rangle$, and $\hat{H}_0|\Psi_y\rangle = E_0|\Psi_y\rangle$. The dipole matrix element is defined as

$$\mathbf{D}_x = \langle\Psi_s|\mathbf{r}|\Psi_x\rangle = D\mathbf{e}_x, \tag{S31}$$

$$\mathbf{D}_y = \langle\Psi_s|\mathbf{r}|\Psi_y\rangle = D\mathbf{e}_y, \tag{S32}$$

where

$$D = \langle \Psi_s | x | \Psi_x \rangle = \langle \Psi_s | y | \Psi_y \rangle. \tag{S33}$$

Inserting all these equations into the TDSE (S28) yields

$$\begin{aligned} i\dot{a}(t) &= [b_1(t)\mathcal{E}_x(t) + b_2(t)\mathcal{E}_y(t)]De^{i(E_s-E_0)t}, & \text{(S34)} \\ i\dot{b}_1(t) &= a(t)\mathcal{E}_x(t)De^{-i(E_s-E_0)t}, & \text{(S35)} \\ i\dot{b}_2(t) &= a(t)\mathcal{E}_y(t)De^{-i(E_s-E_0)t}. & \text{(S36)} \end{aligned}$$

Then, we solve these differential equations numerically, with initial conditions $a(t=0)=0$, $b_1(t=0)=1/\sqrt{2}$ and $b_2(t=0)=i/\sqrt{2}$ for the initial p_+ orbital or $b_1(t=0)=1/\sqrt{2}$ and $b_2(t=0)=-i/\sqrt{2}$ for the initial p_- orbital. After obtaining $b_1(t)$ and $b_2(t)$, we can calculate the projections of the time-dependent wave function onto the $|\Psi_\pm\rangle$ states with

$$b^\pm(t) = \langle \Psi_x \pm i\Psi_y | \Psi(t) \rangle = \langle \Psi_x | \Psi(t) \rangle \mp i \langle \Psi_y | \Psi(t) \rangle = b_1(t) \mp i b_2(t). \tag{S37}$$

III. SEMI-ADIABATIC IONIZATION RATE

In the present work, the semi-adiabatic formula for the instantaneous ionization rates for the deforming p orbitals in elliptically polarized (EP) laser fields is based on the PPT theory for circularly polarized (CP) laser fields [1].

Under the counterclockwise CP field with the angular frequency ω and strength $\mathcal{E}$, the approximate formula for the cycle-averaged ionization rates for $p_\pm$ orbitals is given by [1]

$$\begin{aligned} w_\pm^{\mathrm{CP}}(\omega,\mathcal{E}) \sim\ & \frac{3I_p}{8\sqrt{2\pi}n_0^{3/2}}\left(1+\frac{1}{\gamma^2}\right)^{3/2} \\ & \times \sum_{n\geq n_0}^{\infty}\left(\sqrt{\frac{\zeta^2+\gamma^2}{1+\gamma^2}} \mp \zeta\right)^2 \frac{1}{\sqrt{1-\zeta}}\left(\frac{1+\gamma^2}{\zeta^2+\gamma^2}\right)^{3/4} \exp\left[-\frac{4n_0}{1+\zeta}\left(\operatorname{artanh}\sqrt{\frac{\zeta^2+\gamma^2}{1+\gamma^2}} - \sqrt{\frac{\zeta^2+\gamma^2}{1+\gamma^2}}\right)\right], \end{aligned} \tag{S38}$$

with

$$\begin{aligned} n_0 &= \frac{\mathcal{E}^2}{2\omega^3} + \frac{I_p}{\omega}, & \text{(S39)} \\ \gamma &= \frac{\omega}{\mathcal{E}}\sqrt{2I_p}, & \text{(S40)} \\ \zeta &= \frac{2n_0}{n} - 1 \in (-1, 1], & \text{(S41)} \end{aligned}$$

where I_p denotes the ionization potential. Since the strength and angular frequency of CP fields are constant, the ionization would take place evenly in time. Therefore, here $w_\pm^{\mathrm{CP}}(\omega,\mathcal{E})$ is also considered as the *instantaneous* ionization rate for $p_\pm$ orbitals in CP fields (Assumption I).

In a very small time interval $(t-\delta t/2, t+\delta t/2)$ of an EP laser field, the electric field can be treated as a fraction of the CP field with the field strength $\mathcal{E}_t = |\mathbf{E}(t)|$ and the angular frequency $\omega_t = \partial\theta_t/\partial t = \epsilon\omega[f(t)\mathcal{E}/\mathcal{E}_t]^2$ (Assumption II), where θ_t is the direction of $\mathbf{E}(t)$. The assumptions indicate that the variation of the field strength is treated adiabatically but the nonadiabatic effect caused by the rotational field is retained. Thus, the instantaneous ionization rate for *pure* $p_\pm$ orbitals in the EP fields can be given by

$$\mu_t^\pm \approx w_\pm^{\mathrm{CP}}(\omega_t, \mathcal{E}_t). \tag{S42}$$

However, due to the orbital deformation induced by the Stark effects, the instantaneous orbital is no longer a pure p_+ or p_- orbital but becomes a superposition of them. Therefore, the instantaneous ionization rate for the deforming orbital should be given in a coherent way:

$$\begin{aligned} \mu_m^{\mathrm{EP}}(t) &\sim \left| b_m^+(t)\sqrt{\mu_t^+}e^{+i\theta_i} + b_m^-(t)\sqrt{\mu_t^-}e^{-i\theta_i}\right|^2 & \text{(S43)} \\ &= |b_m^+(t)|^2\mu_t^+ + |b_m^-(t)|^2\mu_t^- + 2|b_m^+(t)||b_m^-(t)|\sqrt{\mu_t^+\mu_t^-}\cos[\Phi_m^+(t) - \Phi_m^-(t) + 2\theta_i]. & \text{(S44)} \end{aligned}$$

Here, $\theta_i = \theta_t + \pi$ is the opposite direction of the instantaneous electric field. $b_m^{\pm}(t) = |b_m^{\pm}(t)| \exp[i\Phi_m^{\pm}(t)]$ are the projections of the time-dependent wave function onto $\Psi_{\pm}^0(\mathbf{r})$, which can be obtained from numerical calculation (three-level model or TDSE). The subscript $m = \pm 1$ denotes the initial $p_{\pm}$ orbitals. The terms $e^{+i\theta_i}$ and $e^{-i\theta_i}$ in Eq. (S43) account, respectively, for the local phases of the p_+ and p_- orbitals at the emitting angle θ_i of the ionizing wave packets.

The physical picture of Eq. (S43) can be interpreted in a transparent way with Eq. (S44). At the time t, the ionizing wave packets are emitted at θ_i from the deforming orbital. The deforming p orbital results essentially from the superposed state of $|\Psi_{p_+}\rangle$ and $|\Psi_{p_-}\rangle$. The wave packets from the overlapping p_+ and p_- orbitals will interfere with each other. The amplitudes of them are $|b_m^{\pm}(t)|\sqrt{\mu_t^{\pm}}$ while the phases of them contain two parts. One is the entire phase shifts of $p_{\pm}$ orbitals, given by $\Phi_m^{\pm}(t)$. The other is the local phases of $p_{\pm}$ at the emitting angle of the ionizing wave packets, given by $\pm\theta_i$. Then, the interference of the wave packets results in the interference term, i.e. the third term, in Eq. (S44).

So far, there is no analytical solution of the complex amplitudes $b_m^{\pm}(t)$ for EP laser pulses. One may need to solve numerically the full 3D TDSE or, simply, the three-level model, as both ways will lead to the close results of $b_m^{\pm}(t)$ for few-cycle pulses.

IV. CLASSICAL BACKPROPAGATION

To extract the initial tunneling exit characteristics, we apply the classical backpropagation method [6, 7] in our numerical simulations. This method does not make any assumption or approximation to the quantum tunneling dynamics, and the tunneling coordinates at the exit is extracted from the final quantum wave packet by transcribing it to the classical phase space and subsequently propagating it backward in time until the classical trajectories reach the tunnel exit.

In Fig. 2 of the main text, we have shown the distribution of the tunneling ionization time obtained by backpropagation. To highlight the difference in the ionization of p_+ and p_- orbitals, we further show in Fig. S1 the distribution of the tunneling exit position of these orbitals. It is clearly seen that the exit position is also rotated between these orbitals. Furthermore, the p_- orbital tunnels out at a position closer to the nucleus because it has a higher total energy at the tunnel exit, which can also be concluded from Fig. S2(a). The higher total energy and the closer exit position of the p_- orbital lead to a higher ionization probability as compared to the p_+ orbital. In addition, the transverse tunneling momentum (momentum perpendicular to the field direction at the tunnel exit within the polarization plane) is also different for p_+ and p_- orbitals. This is illustrated in Fig. S2(b). The transverse momentum is defined as positive when the ionizing electron co-rotates with the electric field.

For the above results as well as that in the main text, we have used the velocity criterion to define the tunnel exit. In other words, we have defined the tunnel exit when the velocity of the classical trajectory in the instantaneous field direction vanishes [6], as defining the tunnel exit via the velocity is necessary to fully and consistently include the nonadiabatic tunneling effects [7].

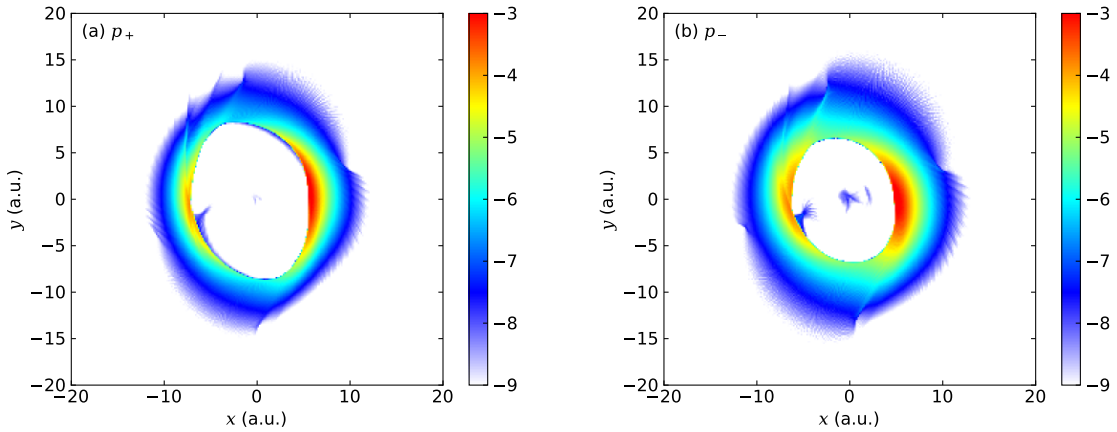

FIG. S1. The distribution of the tunneling exit position of the (a) p_+ and (b) p_- orbitals of the model neon atom.

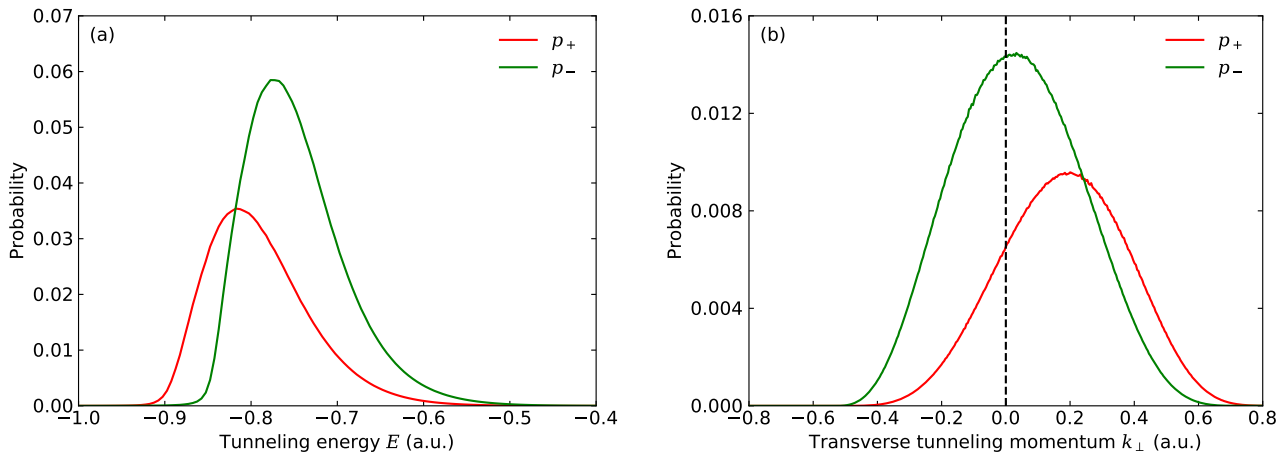

FIG. S2. The distribution of (a) the tunneling energy (total energy at the tunnel exit) and (b) the transverse tunneling momentum (velocity at the tunnel exit perpendicular to the instantaneous field direction in the polarization plane) of the p_+ and p_- orbitals of the model neon atom.

[1] I. Barth and O. Smirnova, Phys. Rev. A **87**, 013433 (2013).
[2] S. Eckart, M. Kunitski, M. Richter, A. Hartung, J. Rist, F. Trinter, K. Fehre, N. Schlott, K. Henrichs, L. P. H. Schmidt, T. Jahnke, M. Schöffler, K. Liu, I. Barth, J. Kaushal, F. Morales, M. Ivanov, O. Smirnova, and R. Dörner, Nat. Phys. **14**, 701(2018).
[3] K. Liu and I. Barth, Phys. Rev. A **94**, 043402 (2016).
[4] M. D. Feit, J. A. Fleck, Jr., and A. Steiger, J. Comput. Phys. **47**, 412 (1982).
[5] X. M. Tong, K. Hino, and N. Toshima, Phys. Rev. A **74**, 031405(R) (2006).
[6] H. Ni, U. Saalmann, and J.-M. Rost, Phys. Rev. Lett. **117**, 023002 (2016).
[7] H. Ni, U. Saalmann, and J.-M. Rost, Phys. Rev. A **97**, 013426 (2018).